

Supporting Information

A new microporous organic-inorganic hybrid titanium phosphate for selective acetalization of glycerol

Bhabani Malakar,^a Sudip Bhattacharjee,^a Nhat Quang Minh Tran,^{b,c} Tan Le Hoang Doan,^{b,c} Thang Bach Phan,^{b,c} Sayantan Chongdar,^a and Asim Bhaumik^{*,a}

^aSchool of Materials Sciences, Indian Association for the Cultivation of Science, Jadavpur, Kolkata 700032, India.

^bCenter for Innovative Materials and Architectures (INOMAR), Ho Chi Minh City, Vietnam

^cVietnam National University-Ho Chi Minh City, Ho Chi Minh City, Vietnam

*Corresponding author. Email: msab@iacs.res.in

Table of contents

Entry	Content	Pages
1	Chemicals	3
2	Synthesis of H-TiPO _x	3
3	Synthesis TiPO _x	3
4	Catalyst characterization	3-4
5	Figure S1: Comparison of PXRD patterns	4
6	Figure S2: Comparison of FTIR spectra	4
7	Figure S3: TGA stability comparison of H-TiPO _x and TiPO _x	5
8	Figure S4: Solid state ³¹ P NMR spectrum of H-TiPO _x	5
9	Figure S5: XPS survey spectrum of H-TiPO _x material	6
10	Figure S6: XPS of Nitrogen 1s in H-TiPO _x material	7
11	Figure S7: XPS of Phosphorous 2p in H-TiPO _x material	7
12	Figure S8: XPS of Oxygen 1s in H-TiPO _x material	8
13	Figure S9: XPS of Carbon 1s in H-TiPO _x material	8
14	Figure S10: HR-TEM images of H-TiPO _x images.	9
15	Figure S11: FE-SEM images and elemental mapping images of H-TiPO _x material	9
16	Table S1: CHN analysis data of H-TiPO _x	10
17	Figure S12: Time dependent ¹ H NMR analysis for glycerol conversion using H-TiPO _x catalyst	10
18	Catalyst reusability studies	10
19	Figure S13: Catalytic reusability after 4th cycle in case of H-TiPO _x	10
20	Hot filtration test	10
21	Figure S14: Catalytic runs and leaching test for H-TiPO _x	11
22	Figure S15: NH ₃ -TPD data of the H-TiPO _x catalysts before and after 4th cycle.	12
23	Figure S16: Powder XRD patterns of the H-TiPO _x catalysts: fresh catalyst and after 4th cycle.	13
24	Figure S17: FT-IR of the H-TiPO _x catalyst before and after 4 th cycle.	13
25	Figure S18: TGA data of the H-TiPO _x catalysts before and after 4th cycle.	13
26	Table S2. Reaction of different aromatic aldehydes with glycerol	13-14
27	Table S3. Comparison of various catalyst used for acetalization of glycerol with acetone	14-15
28	References	16

1. Experimental section

Chemicals

5-aminosalicylic acid and salicylic acid were purchased from Spectrochem, Mumbai. Phosphoric acid (H_3PO_4) was purchased from TCI Chemicals, India; Titanium (IV) isopropoxide was bought from Sigma-Aldrich St. Louis, MO, USA; isopropyl alcohol was obtained from Merck, Bengaluru, India; glycerol was acquired from Bengal Chemicals (Kolkata, India); acetone was bought from Finar Chemicals (Mumbai, India); and the NMR solvent CDCl_3 was purchased from Sigma-Aldrich (USA). Without performing any additional purification, every reagent and solvent was utilized.

Synthesis of H-TiPO_x

Organic-inorganic hybrid titanium phosphate **H-TiPO_x** was synthesized using an organic molecule (5-aminosalicylic acid, 5-ASA) via hydrothermal method.¹ At first, 664 mg of 5-amino-2-hydroxybenzoic acid was dissolved in 10 mL distilled water, and then 1 g of 85% phosphoric acid was mixed to it and the mixture was stirring for 2 h. In a separate glass vial, 2.465 g of titanium isopropoxide was dissolved in 3-4 mL isopropyl alcohol. Then this titanium isopropoxide solution was added to the previous solution under vigorous stirring conditions. For 15 to 20 minutes, the final mixture was vigorously stirred at room temperature. Finally, the solution was transferred to a stainless-steel-coated Teflon-lined autoclave of volume 50-mL and kept static for 48 hours at 150 °C in a hot air oven. Then the container was cooled, and the white precipitate was washed with plenty of water, followed by methanol, ethanol, and THF. Finally, the product was dried at 80 °C under vacuum. The material was then characterized using several techniques.

Synthesis TiPO_x

Titanium phosphate **TiPO_x** was synthesized by hydrothermal method. In a 50 mL RB 10 mL distilled water and 1 g of 85% phosphoric acid was taken. The solution was stirred for half an hour at room temperature. In a separate glass vial, 2.465 g of titanium isopropoxide was dissolved in isopropyl alcohol. Then this titanium isopropoxide solution was added dropwise to the previous solution under vigorous stirring conditions. After the addition was completed, the final solution was stirred for 20 minutes. Then the solution was transferred to a stainless-steel-coated Teflon-lined autoclave with a 50-mL volume capacity and kept static for 48 hours at 150 °C in a hot air oven. The container was then cooled, and the white precipitate was obtained, which was washed with water, followed by ethanol, and THF. Finally, the product was dried at 80 °C under vacuum and powder X-ray diffraction experiment was performed. For the synthesis of **Sal-TiPO_x** identical synthesis procedure is followed as that of H-TiPO_x except replacing 5-ASA by salicylic acid.

2. Catalyst characterization:

Crystalline nature of the both the materials were studied using a Bruker AXS D8 Advanced SWAX diffractometer connected to a nickel-filtered $\text{Cu K}\alpha$ ($\lambda = 0.15406$ nm) radiation source at an operating at 40 kV in the range of 2-40°. The surface area of the titanium phosphate material was explored by exploring the Brunauer-Emmett-Teller (BET) surface through N_2 sorption analysis at 77 K using a Quantachrome Autosorb iQ surface area analyzer (Quantachrome Inc., Boynton Beach, FL, USA). In order to perform the experiment, the sample was kept at 85 °C oven before being degassed at a temperature of 120 °C for three hours under continuous vacuum. The non-local density functional theory (NLDFT) approach was used to study the pore size distribution. The bonding connectivity of both the materials were analyzed using Fourier transform infrared (FTIR) spectroscopy in the range of 400-4000 cm^{-1} using KBr pellets. FTIR analysis was performed using a PerkinElmer, Cambridge, MA, USA, spectrophotometer. To examine the morphology of hybrid titanium phosphate sample field-emission scanning electron microscopy (FE-SEM) experiments were performed on JEOL JEM 6700F. High-resolution transmission electron microscopic analysis of the hybride titanium phosphate material was carried out using JEOL JEM 2100F, Japan, equipment working from a 200-kV electron source. For the TEM experiment, the sample was dispersed in methanol and drop-casted on a carbon-coated copper grid. Ultrahigh-resolution transmission electron microscopy images were analyzed in order to learn more about the morphological examination of the materials. Elemental analyses (C, H and N) were performed using a CHN analyzer Perkin-Elmer 2400 series-II. NMR spectrum was recorded on Bruker 600 MHz spectrometer using tetramethylsilane as an internal reference. TGA experiment of both the TiPO material were carried out in synthetic air ($100 \text{ cm}^3 \text{ min}^{-1}$) using a NETZSCH STA 449F3 Jupiter thermal analyzer. The TGA instrument was equipped with a QMS 403 Aëolos mass spectrometer for evolved gases (EGA). The experiment was conducted in an open crucible made of $\alpha\text{-Al}_2\text{O}_3$, from 30 °C to 800 °C, with a heating rate of 10 °C min^{-1} . The temperature-programmed desorption analysis of NH_3 ($\text{NH}_3\text{-TPD}$) was collected on the AMI-300 Lite Chemisorption Analyzer TPR/TPD of Altramira Instruments LLC, USA, with a thermal conductivity detector (TCD). Prior to the TPD measurement, the sample (~0.15 g) was pre-processed at 500 °C for 1 h under He gas ($50 \text{ mL}\cdot\text{min}^{-1}$) and then cooled to 100 °C. After that, the sample was saturated with NH_3 (10 mol% $\text{NH}_3\text{-He}$ gas for 30 min with $50 \text{ mL}\cdot\text{min}^{-1}$)

then, the sample was treated with He at 100 °C for 30 min to remove the physically absorbed NH₃ molecules. Finally, the sample was heated to 600 °C with a heating rate of 10 °C·min⁻¹.

Rietveld refinements:

Rietveld refinements were conducted using the MAUD software, adhering to the criteria outlined by Lutterotti, with an acceptable R_w value of less than 15%. Our refinement achieved a R_w value of 6.28%, meeting the required criteria and demonstrating a high level of accuracy. The refined parameters can now be analyzed in depth to gain insight into the crystallographic structure of the materials. R_w is calculated by this equation:

$$R_w = \sqrt{\frac{\sum_i w_i (y_{c,i} - y_{o,i})^2}{\sum_i w_i (y_{o,i})^2}}$$

Where $y_{c,i}$ is the calculated intensity for a given data point; $y_{o,i}$ is the specific intensity of a given data point as measured. And w_i is defined as:

$$w_i = \frac{1}{\sigma^2(y_{o,i})}$$

With σ is defined as the standard deviation for a specific intensity value $y_{o,i}$.

The structural parameters offer crucial insights into the crystalline nature of the material. By refining experimental data against a simulated structure based on the unit cell formula of approximately Ti₆P₇O₃₇C₁₄N₂H₁₅. Employing Le Bail's approach, the measured intensity data were meticulously analyzed, enabling precise determination of the material's atomic arrangement. This method utilized the intensity of indexed peaks in the powder sample diffraction data to extract accurate structural information. The close agreement between the experimental PXRD pattern and the simulated diffraction pattern underscores the success of the synthesis process, indicating the acquisition of the target material with the desired crystalline structure. This comprehensive approach not only provides valuable structural parameters but also validates the synthesis success, laying a solid groundwork for further analysis and applications.

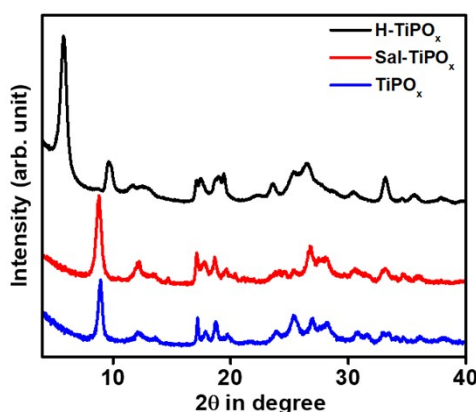


Figure S1: PXRD patterns of H-TiPO_x (synthesized by using 5-ASA), Sal-TiPO_x (synthesized by using salicylic acid) and TiPO_x (no organic) materials.

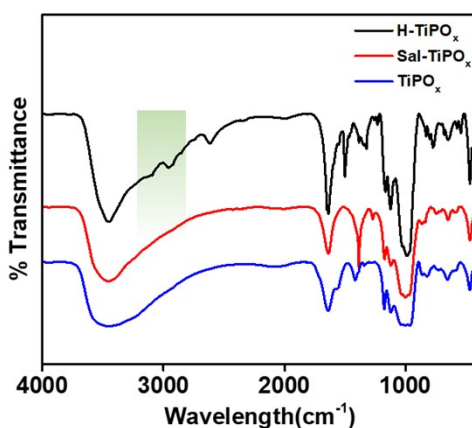


Figure S2: FTIR spectra of H-TiPO_x (synthesized by using 5-ASA), Sal-TiPO_x (synthesized by using salicylic acid) and TiPO_x (no organic) materials.

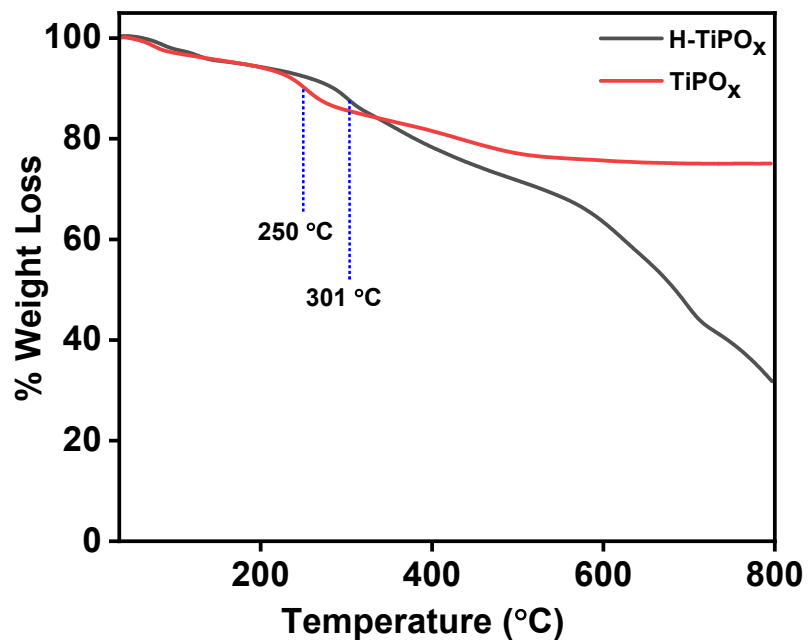


Figure S3: TGA stability comparison of H-TiPO_x and TiPO_x.

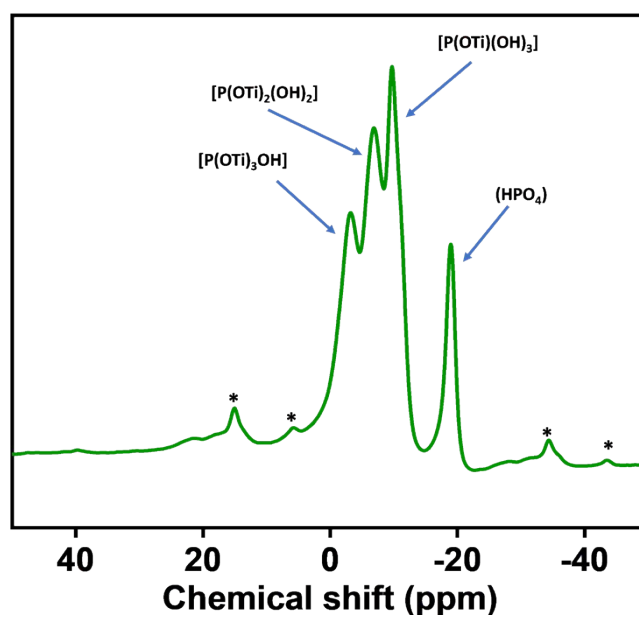


Figure S4: Solid state ³¹P NMR spectrum of H-TiPO_x.

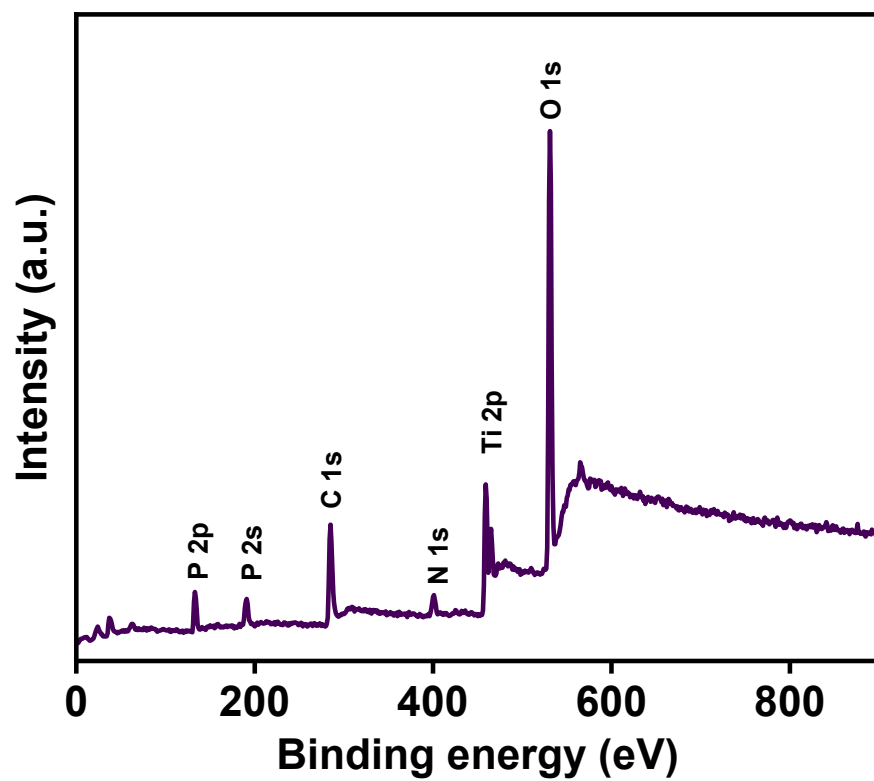


Figure S5: XPS survey spectrum of H-TiPO_x.

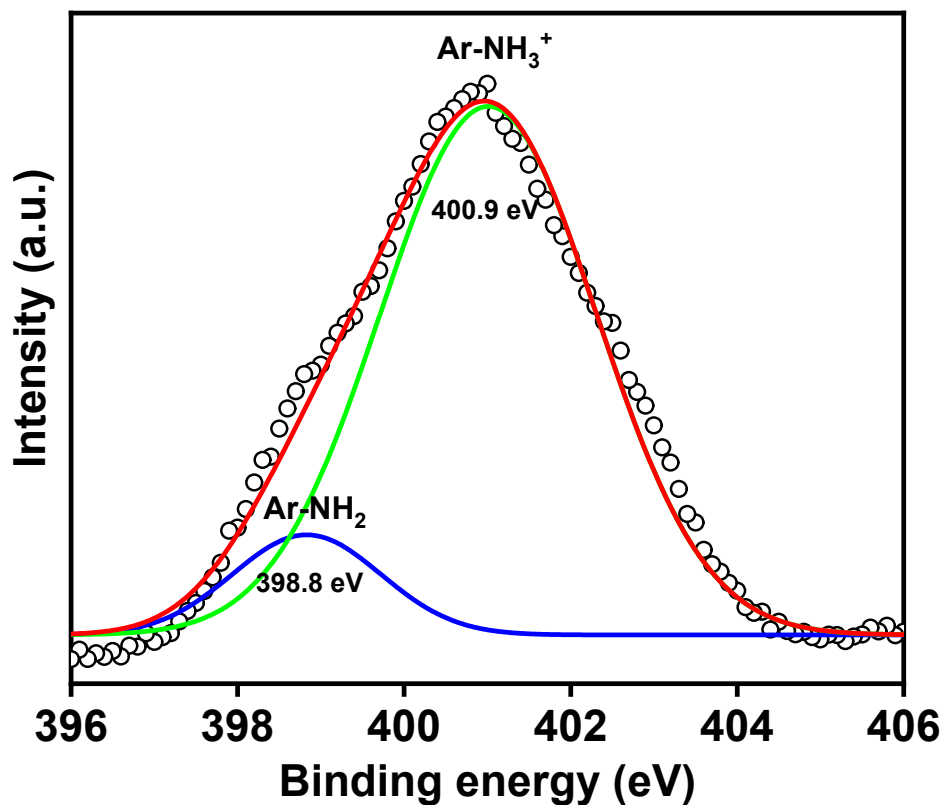


Figure S6: XPS of Nitrogen 1s in H-TiPO_x material.

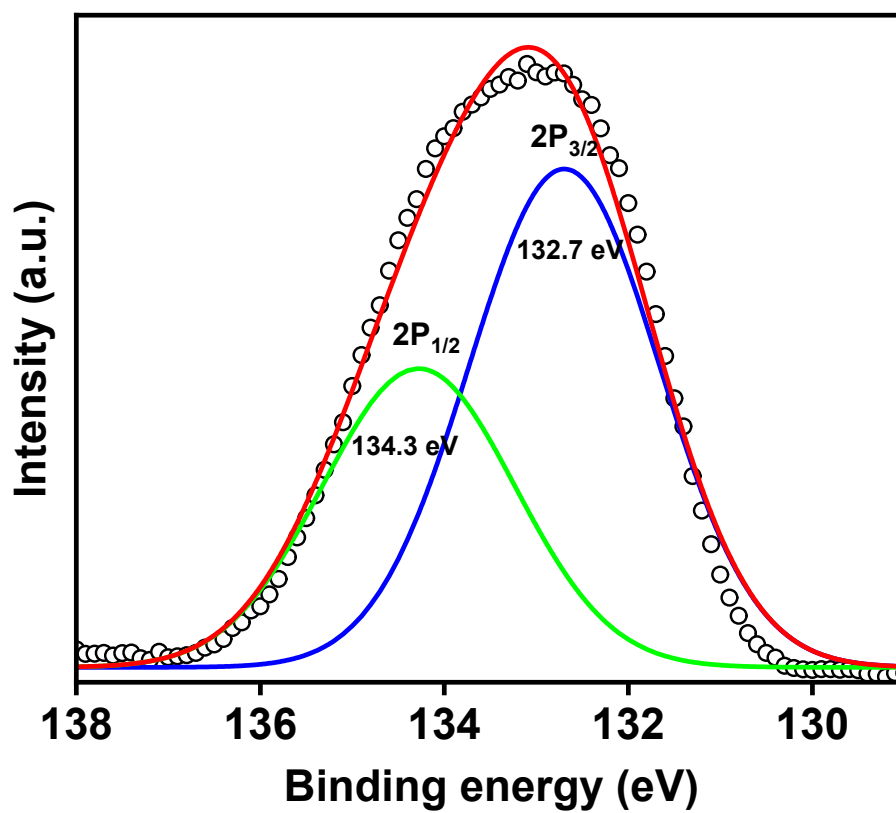


Figure S7: XPS of Phosphorous 2p in H-TiPO_x material.

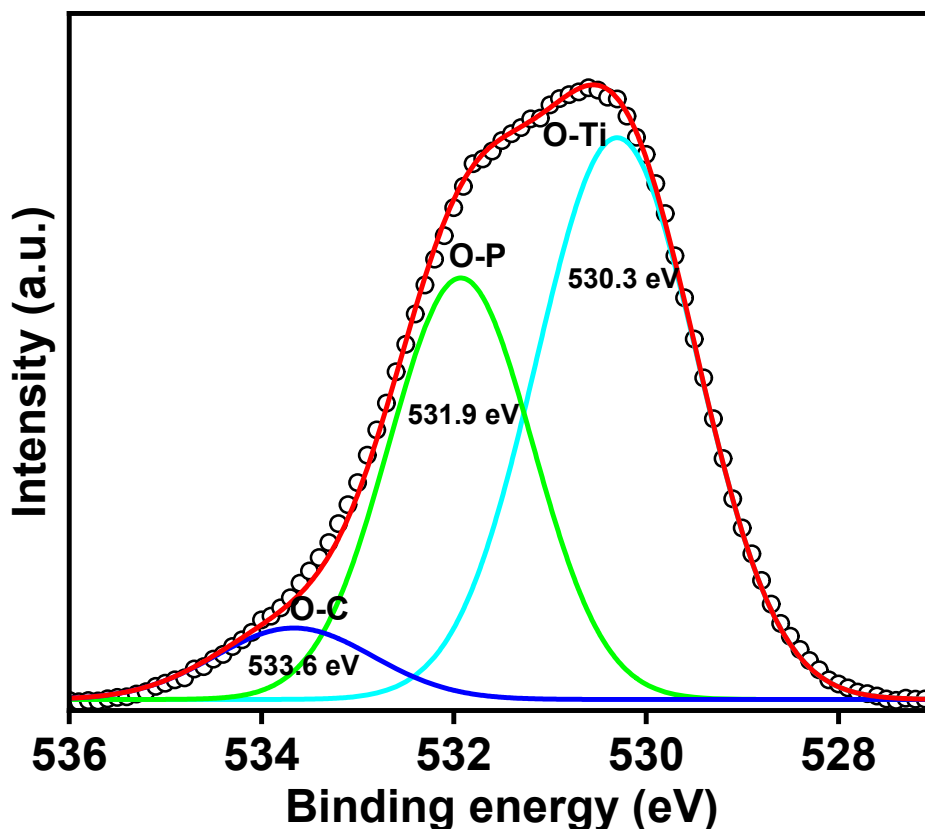


Figure S8: XPS of oxygen 1s in H-TiPO_x material.

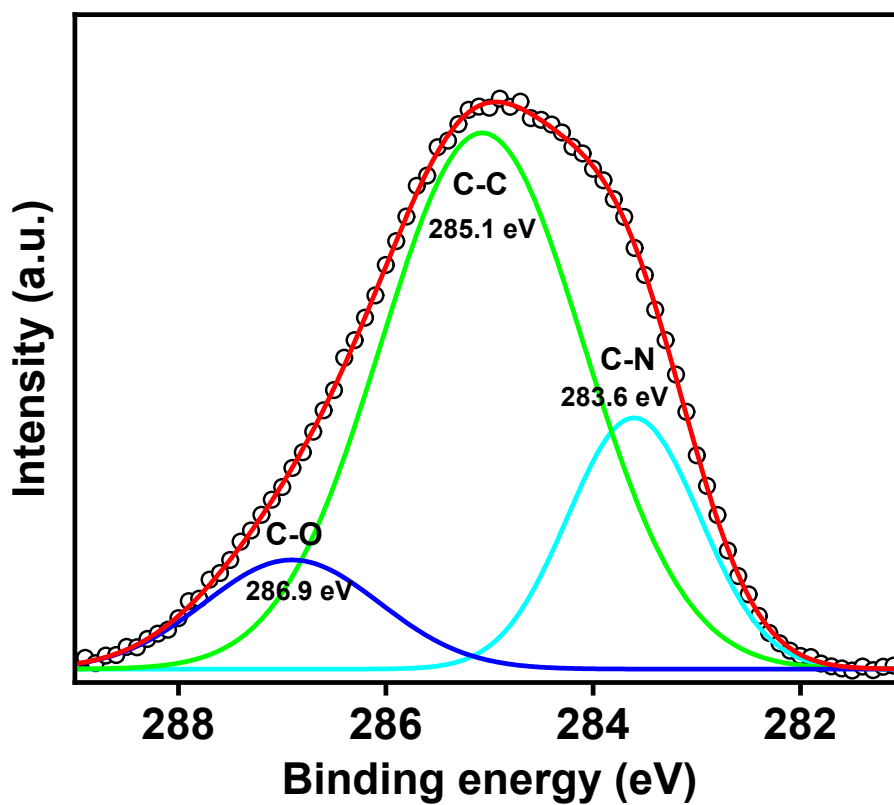


Figure S9: XPS of carbon 1s in H-TiPO_x material.

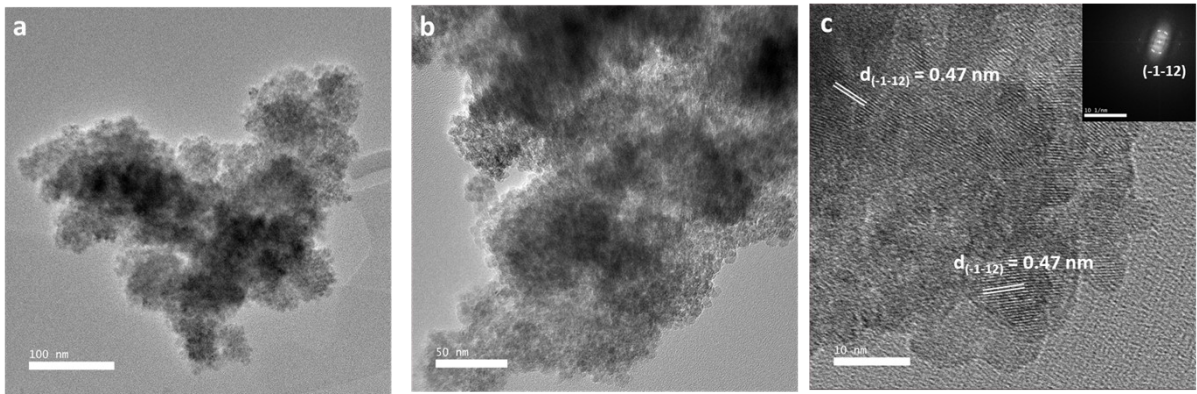


Figure S10: HR-TEM images of H-TiPO_x images.

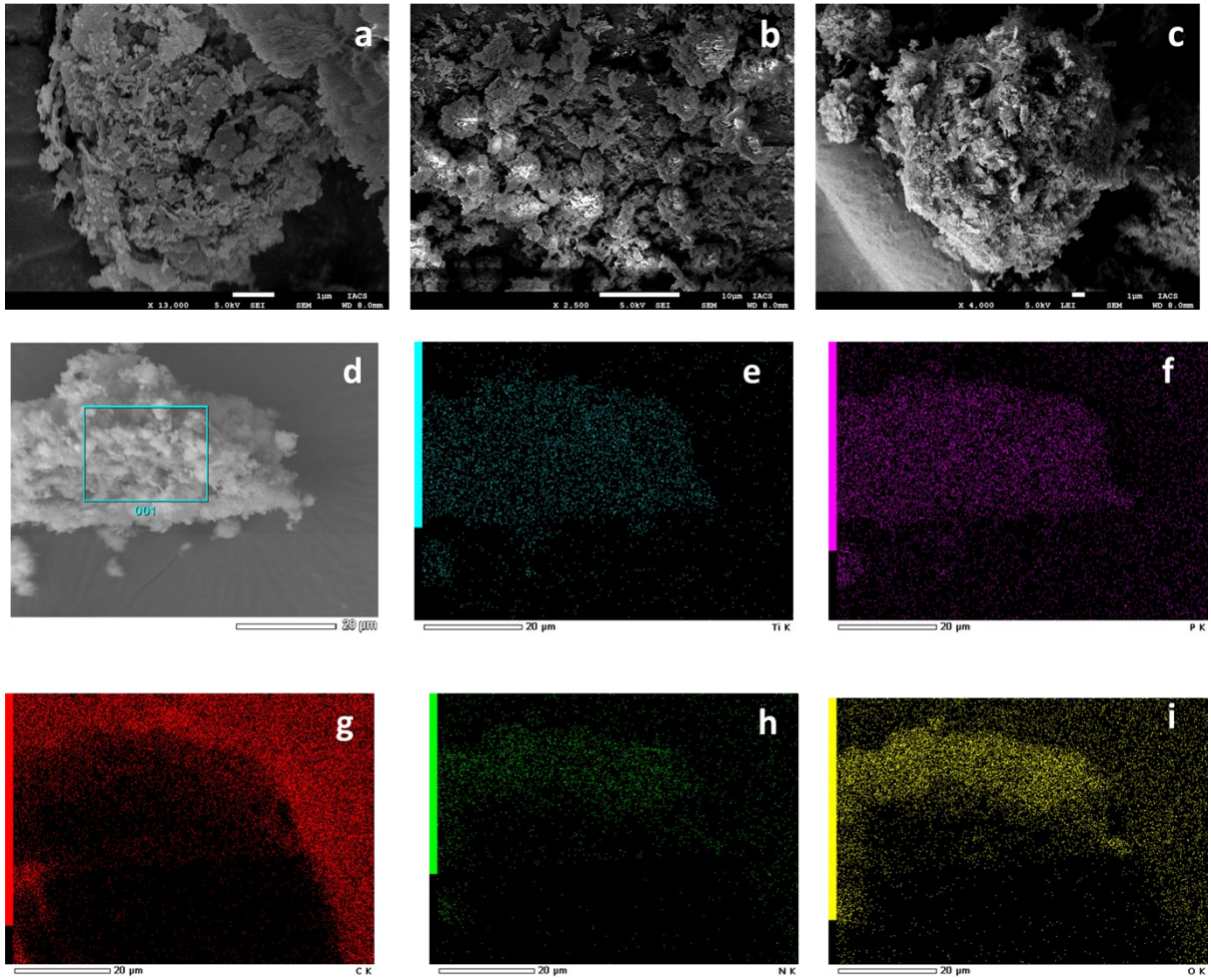


Figure S11: FE-SEM images and elemental mapping images of H-TiPO_x material.

Table S1: CHN analysis data of H-TiPO_x material.

Element	Before Catalysis (%)	After Catalysis (%)
Carbon	9.81	9.84
Hydrogen	0	0.90
Nitrogen	1.56	1.56

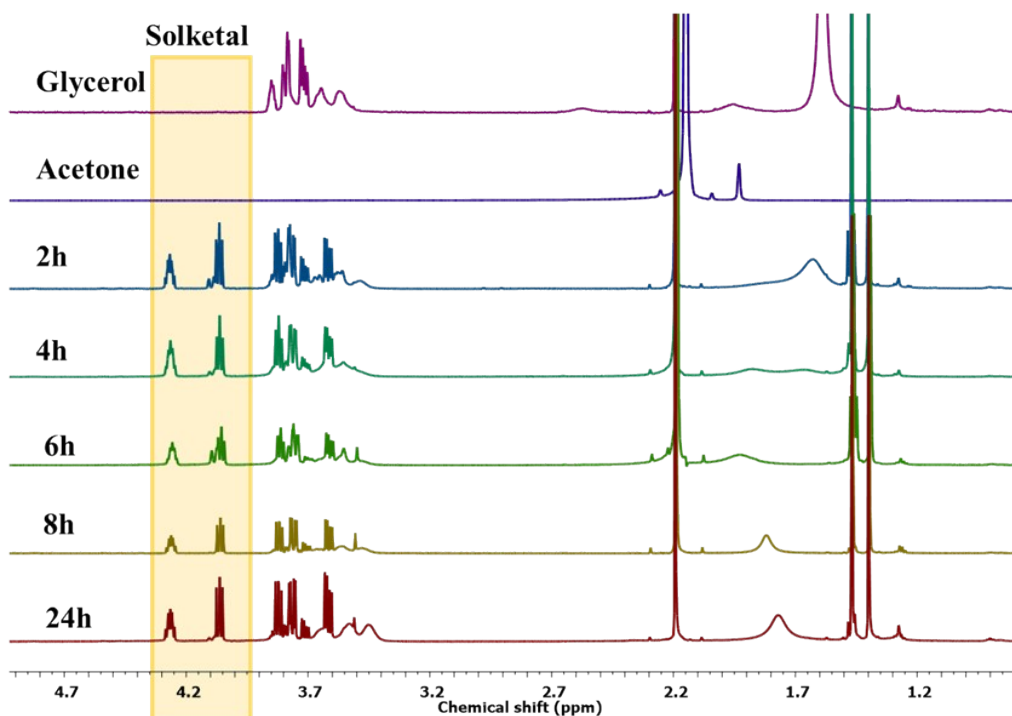


Figure S12: Time dependent ¹H NMR analysis for glycerol conversion using H-TiPO_x catalyst.

Catalyst reusability studies

To explore the stability of the catalyst, recyclability test of glycerol acetalization were carried out on the H-TiPO_x catalyst. The used catalyst was collected by centrifugation and washed several times with water and methanol to remove the impurities from the catalyst surface. After that, it is dried in an oven at 100 °C for 2-3 hours. The recycled catalyst was also subjected to PXRD, and FT-IR analysis (Figure S8 and S9). PXRD and FTIR results showed no significant changes in the properties of the reused catalyst compared to the fresh catalyst. Then the catalyst was reused for another catalytic experiment. This procedure was repeated three times for successive recycles. The conversion of glycerol was decreased very little amounts after successive reuses of the catalyst, which indicates a slight decline in the activity of the catalyst due to the blockage of acidic sites. However, selectivity remains almost unchanged, which suggests the robustness of the catalyst surface and framework.

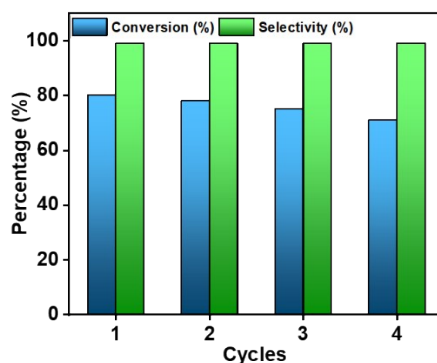
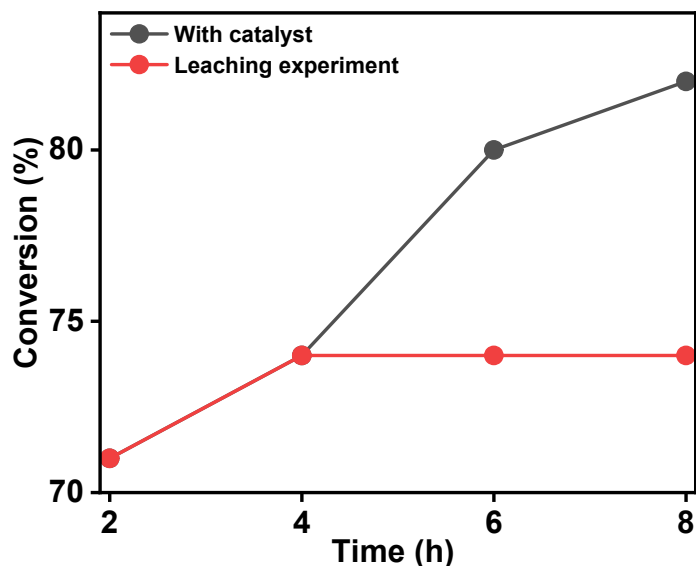


Figure S13: Catalytic reusability after 4th cycle in case of H-TiPO_x.

Hot filtration test: To understand the heterogeneous nature of H-TiPO_x catalyst, the leaching test was carried out in accordance with the hot filtration method. For this process, we carried out the reaction under optimum conditions. Then the reaction was stopped after 4 hours and the catalyst was separated from the reaction mixture by centrifugation. The yield of the product was 71% calculated through ^1H NMR. Next, the reaction was further continued for up to 8 hours under catalyst-free conditions. From Figure S14, it can be seen that the yield was maintained. It was observed that after catalyst separation, there was no significant increase in yield, implying that the active sites were intact in the catalyst and there was no leaching



of active metal (Ti) from the catalyst.

Figure S14: Catalytic runs and leaching test for H-TiPO_x .

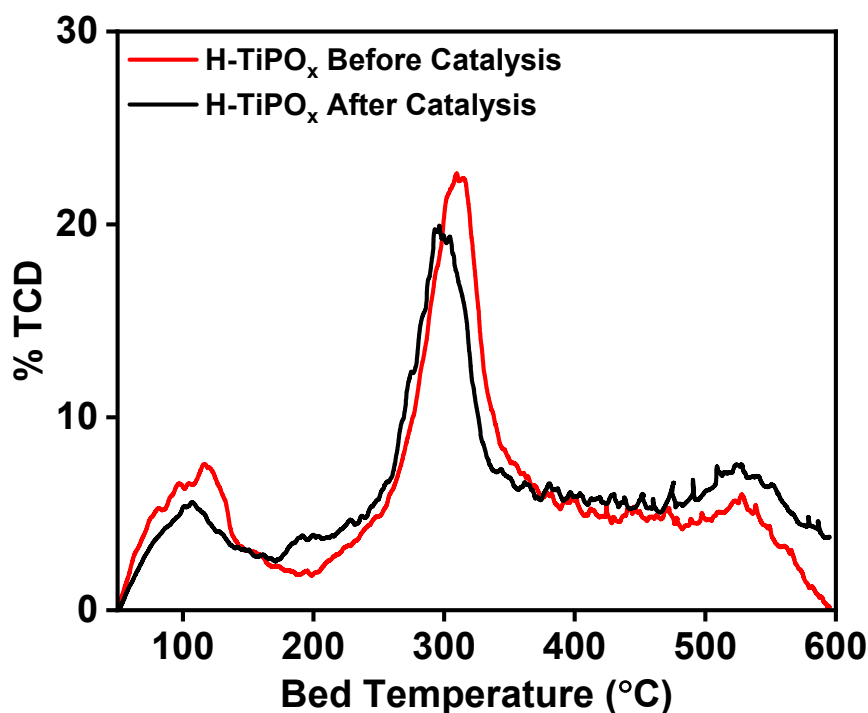


Figure S15: NH_3 -TPD data of the H-TiPO_x catalysts before and after 4th cycle.

The surface acidity of the reused **H-TiPO_x** catalyst after fourth cycle was determined from the NH_3 -TPD (NH_3 -temperature-programmed desorption) analysis (Fig. S15). The total surface acidities of **H-TiPO_x** before and catalysis after four cycle were found to be 5.9 and 5.3 mmol g^{-1} , respectively.

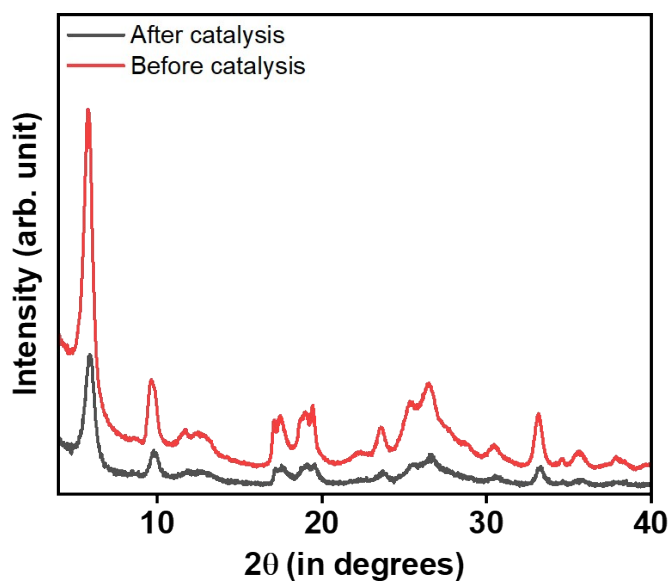


Figure S16: Powder XRD patterns of the **H-TiPO_x** catalysts before and after 4th cycle.

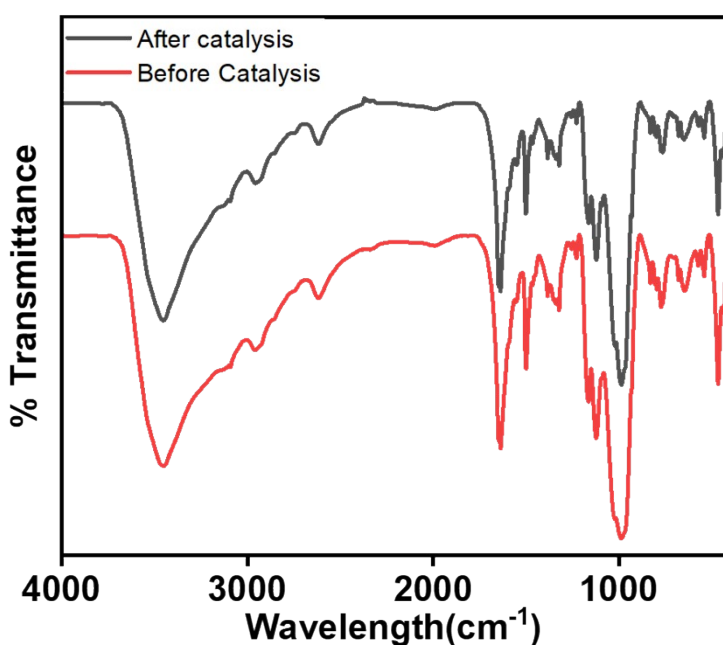


Figure S17: FT-IR spectra of the **H-TiPO_x** catalysts before and after 4th cycle.

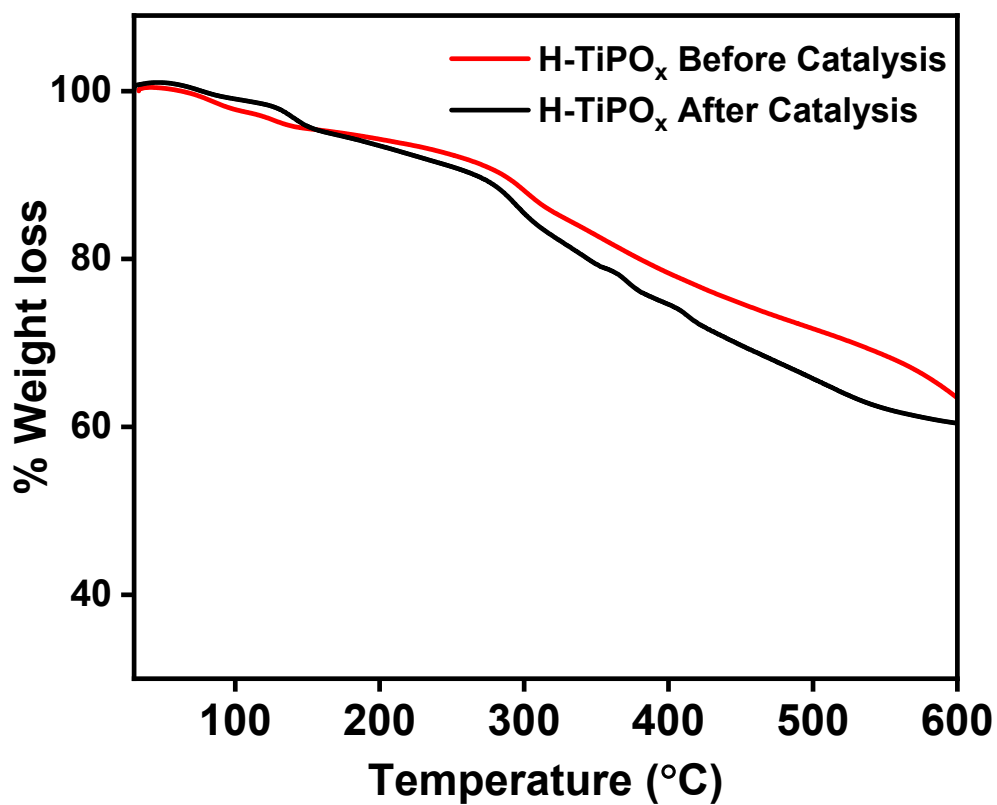
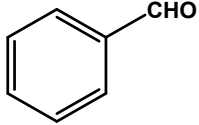
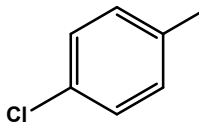
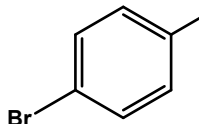
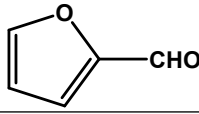
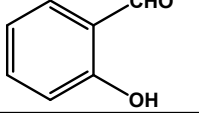
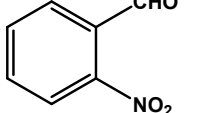


Figure S18: TGA data of the fresh and used H-TiPO_x catalysts after 4th reaction cycle.

Table S2: Reaction of different aromatic aldehyde with glycerol catalysed by H-TiPO_x

Sl. No.	Substrate	Conversion (%)	5/6 Member selectivity
1		73%	1
2		84%	0.85
3		80%	3.16
4		82%	2.84
5		63%	0.63
6		88%	0.64

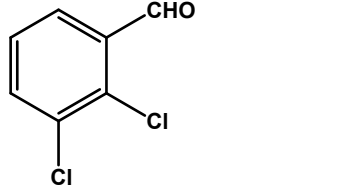
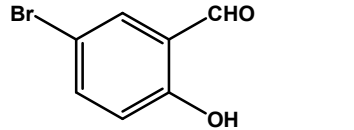
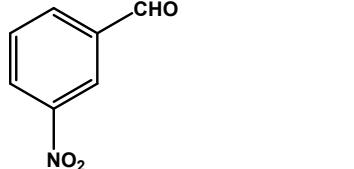
7		40%	0.81
8		81%	0.42
9		76.85%	0.67

Table S3: Comparison of various heterogeneous catalysts used for acetalization of glycerol with acetone

Sl. No	Name	Condition	Surface Area (m ² /g)	Acidity (mmol/g)	Selectivity	Conversion (%)	TON ¹	TOF (h ⁻¹) ²	Ref.
1	HZSM-5	10.86 mmol glycerol, 108.6 mmol acetone, 0.05 g catalyst, 25 °C, 1.5 h.			65.4	7.2	0.9	0.6	2
2	HBEA	Same as above	500	0.87	97.5	70.9	13.2	8.8	2
3	Amberlyst-45	Same as above			97.4	80.6	15.0	10	2
4	H ₃ PW ₁₂ O ₄₀	Same as above			98.6	84.5	15.9	10.6	2
5	PSF/K-SiO ₂	Same as above	77.8	2.6	97.7	86.3	16.1	10.7	2
6	C-SO ₃ H	10.86 mmol glycerol, 65.2 mmol acetone, 0.05 g catalyst, 40 °C, 1 h			99.5	94.0	26.8	26.8	3
7	Acid carbon catalyst	10.1 mmol glycerol, 39.6 mmol acetone, 0.028 g catalyst, 25 °C, 4 h	10	3.8	95.0	80.0	9.1	2.3	4
8	Hollow sphere carbon-SO ₃ H	10 mmol glycerol, 10 mmol acetone, 0.05 g catalyst, 80 °C, 6 h.			99.2	79.1	3.5	0.6	5
9	WO ₃ /SnO ₂	Glycerol/Acetone (1/1), 1.5 h, RT	32	0.06	96	55	-	-	6
10	MO ₃ /SnO ₂	Glycerol/Acetone (1/1), 2.5 h, RT	56	0.08	96	71	154.5	103	6
11	NbO ₂ OH	Glycerol/Acetone (1/4), 1 h, 70 °C	135	0.09	95	73	-	-	7
12	H ₃ PW ₁₂ O ₄₀	Glycerol/Acetone (1/20), 2 h, RT			98	83	-	-	8
13	Montmorillonite k10	Glycerol/Acetone (1/20), 2h, Refluxed	233	0.28	99	83	-	-	9
14	Sn-MCM-41	Glycerol/Acetone (1/1), 6 h, 80 °C	724	0.011	100	40	-	-	10

15	Zr-TUD-1	Glycerol/Acetone (1/1), 6 h, 80 °C,	651	0.16	100	46	-	-	10
16	Hf-TUD-1	Glycerol/Acetone (1/1), 6 h, 80 °C	715	0.27	100	52	234	39	10
17	Al-SBA-15	Glycerol/Acetone (1/1), 8 h, 100 °C	720	0.14	99	75	-	-	11
18	PSF polymer	Glycerol/Acetone (1/5), 4h, 60 °C 8% cat	59.78	0.65	100	97	14.1	-	12
19	Nb ₂ (OH)	Glycerol/Acetone (1/2), 1h, 70 °C 8% cat 200mg	34	0.23	95	65	33	33	13
20	Nb ₂ O ₅	Glycerol/Acetone (1/1.5), 6h, 70 °C 6.4 wt% cat	121	4.7	92	80	138	23	14
21	Ar-SBA-15	Glycerol/Acetone (1/6), 0.5h, 70 °C 5wt% cat			-	80	17.4	-	15
22	Al(TF)-MCM-41	Glycerol/Acetone (1/4), 4 h, RT, 8 wt %	817	3.02	100	86	92	23	16
23	Sn ₄ ²⁺ /SnO ₂	Glycerol/Acetone (1/1), 4 h, RT, 5 wt %	11	0.046	96	95	208	52	17
24	Activated carbon–SO ₃ H	Glycerol/Acetone (1/4), 6 h, RT, 2.7 wt %			96	97	-	65	18
25	Sulfonated polymer	Glycerol/Acetone (1/5), 0.5 h, RT, 0.5 wt %	340	1.7	98	94	-	-	19
26	GS-SO ₃ H	Glycerol/Acetone (1/4), 4 h, RT, 5 wt %	471	5.45	98	91	200	50	20
27	Amberlyst-36	40 °C	19	5.4	100	88	-	-	21
28	Amberlyst-15	70 °C	50	4.2	100	95	-	-	22
29	zeolite beta	35 °C			100	98	-	-	23
30	Hybrid Titanium Phosphate, H-TiPO_x	Glycerol/Acetone (1/4), 8 h, room temperature	97	5.9	99	84	51.6	6.5	This work

¹TON: Turn over number (moles of substrate converted per mole of the catalyst)

²TOF: Turn over frequency (moles of substrate converted per mole of the catalyst per hour)

References

1. C. Nan, J. Lu, C. Chen, Q. Peng and Y. Li, *J. Mater. Chem.*, 2011, **21**, 9994-9996.
2. R. Zhou, Y. Jiang, H. Zhao, B. Ye, L. Wang and Z. Hou, *Fuel*, 2021, **291**, 1-9.
3. L. J. Konwar, A. Samikannu, P. Mäki-Arvela, B. Dan and J. P. Mikkola, *Appl. Catal., B Environ*, 2018, **220**, 314-323.
4. M. Gonçalves, R. Rodrigues, T. S. Galhardo and W. A. Carvalho, *Fuel*, 2016, **181**, 46-54.
5. L. Wang, J. Zhang, S. Yang, Q. Sun, L. Zhu, Q. Wu, H. Zhang, X. Meng and F.-S. Xiao, *J. Mater. Chem. A*, 2013, **1**, 9422-9426.

6. B. Mallesham, P. Sudarsanam, G. Raju and B. M. Reddy, *Green Chem.*, 2013, **15**, 478-489.
7. T. E. Souza, I. D. Padula, M. M. Teodoro, P. Chagas, J. M. Resende, P. P. Souza and L. C. Oliveira, *Catal. Today*, 2015, **254**, 83-89.
8. M. J. da Silva, A. A. Julio and F. C. S. Dorigetto, *RSC Adv.*, 2015, **5**, 44499-44506.
9. J. Deutsch, A. Martin and H. Lieske, *J. Catal.*, 2007, **245**, 428-435.
10. L. Li, T. I. Koranyi, B. F. Sels and P. P. Pescarmona, *Green Chem.*, 2012, **14**, 1611-1619.
11. C. Gonzalez-Arellano, R. A. D. Arancon and R. Luque, *Green Chem.*, 2014, **16**, 4985-4993.
12. I. B. Laskar, K. Rajkumari, R. Gupta and L. Rokhum, *Energy Fuels*, 2018, **32**, 12567-12576.
13. T. E. Souza, M. F. Portilho, P. M. T. G. Souza, P. P. Souza and L. C. A. Oliveira, *ChemCatChem*, 2014, **6**, 2961-2969.
14. G. S. Nair, E. Adrijanto, A. Alsalmeh, I. V. Kozhevnikov, D. J. Cooke, D. R. Brown and N. R. Shiju, *Catal. Sci. Technol.*, 2012, **2**, 1173-1179.
15. G. Vicente, J. A. Melero, G. Morales, M. Paniagua and E. Martin, *Green Chem.*, 2010, **12**, 899-907.
16. K. N. Tayade, M. Mishra, M. K. and R. S. Somani, *Catal. Sci. Technol.*, 2015, **5**, 2427-2440.
17. B. Mallesham, P. Sudarsanam and B. M. Reddy, *Catal. Sci. Technol.*, 2014, **4**, 803-813.
18. R. Rodrigues, M. Gonçalves, D. Mandelli, P. P. Pescarmona and W. A. Carvalho, *Catal. Sci. Technol.*, 2014, **4**, 2293-2301.
19. S. R. Churipard, P. Manjunathan, P. Chandra, G. V. Shanbhag, R. Ravishankar, P. V. Rao, G. S. Ganesh, A. Halgeri and S. P. Maradur, *New J. Chem.*, 2017, **41**, 5745-5751.
20. A. Ghosh, A. Singha, A. Auroux, A. Das, D. Sen and B. Chowdhury, *Catal. Sci. Technol.*, 2020, **10**, 4827-4844.
21. A. Sokołowski, A. Piasecki and B. Burczyk, *J. Am. Oil Chem. Soc.*, 1992, **69**, 633-638.
22. J. Deutsch, A. Martin and H. Lieske, *J. Catal.*, 2007, **245**, 428-435.
23. C. X. A. da Silva, V. L. C. Gonçalves and C. J. A. Mota, *Green Chem.*, 2009, **11**, 38-41.